Evaluation of A Ku-band Radar Hydrometeor Classifier by Comparison with S-band Radar and Aircraft Data

Haonan Chen* and V. Chandrasekar
Colorado State University, Fort Collins, CO, USA
*haonan.chen@colostate.edu

***Abstract*—Compared to traditional single-polarization radar, dual-polarization radar can provide more information about different hydrometeor sizes, shapes and their distribution. However, most of the previous studies were devoted to S or C band frequencies since they are standard operating frequencies in many countries. In this paper, we demonstrate the application of Ku-band dual-polarization radar for hydrometeor identification. The derived hydrometeor types are cross compared with collocated S-band products and images collected by the airborne probe. Results show that the Ku-band radar has great potential for characterization of precipitation microphysics and identifying different hydrometeor phases.**

I. INTRODUCTION

Dual-polarization weather radars have been widely used for rainfall estimation and studies of precipitation microphysics (e.g., [1]). A number of previous studies have already demonstrated that the dual polarization radar measurements can be used to identify different hydrometeor types and retrieve the hydrometeor particle size distribution. Nevertheless, most of the previous research focused on S- or C- band frequencies since they are standard operating frequencies in many countries. In recent years, dense radar network at X-band, especially for urban deployment, is gaining increasing interest because of the cost efficiency and portability [2]. However, the research at higher frequencies such as Ku and Ka band is relatively rare.

In order to validate the Global Precipitation Measurement (GPM) satellite measurements and products [3], NASA has developed a Dual-frequency, Dual-polarization, Doppler Radar (D3R) as part of the ground validation (GV) activities. The Ku- and Ka-band D3R is analogous to the GPM core satellite dual-frequency precipitation radar, but can provide more detailed insight into the precipitation microphysics through the ground-based dual-frequency dual-polarization measurements. The D3R has substantively participated in GPM GV field campaigns covering different geographic features and in both winter and summer conditions[4-8].

This paper presents the application of Ku-band dual-polarization radar for hydrometeor classification. The differential phase based attenuation correction for Ku-band observations, as well as the region-based hydrometeor classifier are detailed. The D3R data collected during the GPM GV field experiments are extensively used for demonstration purposes. The D3R's hydrometeor classification products are evaluated through cross-comparison with *in situ* aircraft data and collocated S-band products.

II. ATTENUATION CORRECTION

At high frequencies such as X-band or higher, radar measurements suffer from attenuation along the propagation paths due to rainfall. Therefore, radar reflectivity and differential reflectivity should be corrected for attenuation before used for any quantitative applications. The specific attenuation resulting from absorption and scattering through propagation in rain at two polarization channels are related to raindrop size distribution as:

$$\alpha_{h,v} = 4.343 \times 10^{-3} \int \sigma_{\text{ext}}(h,v) N(D) dD \qquad (1)$$

where σ_{ext} is the extinction cross section derived by the sum of the absorption and scattering cross section; D is the volume equivalent spherical diameter; $N(D)$ represents the raindrop size distribution.

In this paper, the differential phase-based approach is implemented for attenuation correction, where a linear relation between specific attenuation $\alpha_{h,v}$ and specific differential phase K_{dp} is assumed and applied to compensate measured reflectivity Z_h and differential reflectivity Z_{dr}. The Z_{dr} vs. Z_h curves in Fig. 1 illustrate the performance of Ku-band attenuation correction. The Ku-band data shown in Fig. 1 were collected by the NASA D3R on November 12, 2015, at 14:34UTC. The red curve shows the Ku-band measurements,

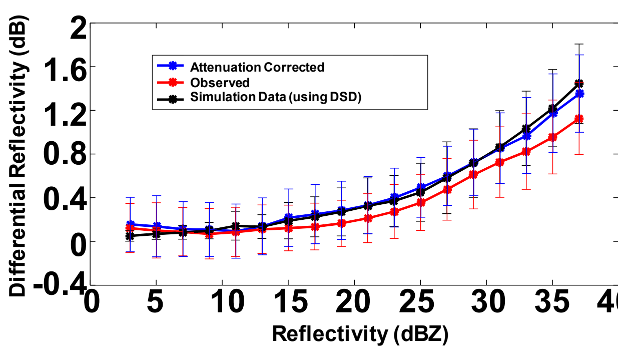

Fig. 1. Z_{dr} vs. Z_h (before and after attenuation correction) for the Ku-band data collected on 12 Nov 2015, at 14:34UTC.

whereas the blue curve illustrates the data after attenuation correction. It should be noted that the simulation data shown in black curve are obtained based on raindrop disdribution (DSD) data through *T*-matrix scattering computation. The DSD data were collected by disdrometers that were deployed under D3R's coverage umbrella. The bars associated with the curves in Fig. 1 represent the standard deviations. Fig. 1 shows that compared with observed data the attenuation corrected measurements match the simulation data very well.

III. Hydrometeor Classification and Evaluation

Traditionally, the fuzzy-logic based approaches are used for hydrometeor classification. However, the bin-by-bin based classification methodology has limitations when applied to "noisy" radar data that could be caused by ground clutter and/or bright band contamination. In this paper, a region-based approach has been implemented at Ku-band. The overall structure of this region-based classification methodology is depicted in Fig. 2. Fig. 3 shows the NASA D3R Ku-band observations and corresponding hydrometeor classification results on June 05, 2013, at 1224UTC. Compared to conventional fuzzy-logic method, this region-based approach is appealing in terms of operational application and easy interpretation. In this study, the Ku-band hydrometeor classifier is evaluated through cross-comparison with collocated S-band products and *in situ* aircraft probe images.

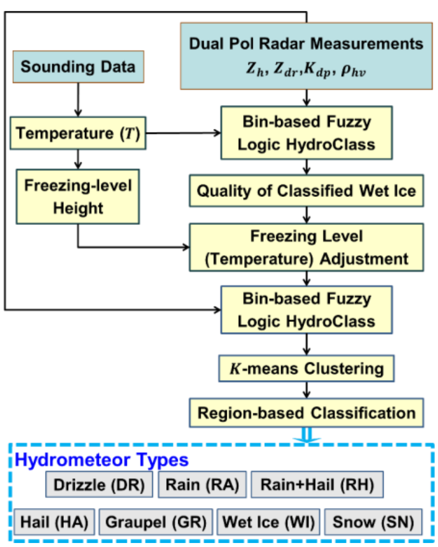

Fig. 2. System diagram of the implemented region-based hydrometeor classification method.

Acknowledgement

This research was supported by the NASA GPM/PMM program.

References

[1] H. Chen, V. Chandrasekar, and R. Bechini, "An Improved Dual-Polarization Radar Rainfall Algorithm (DROPS2.0): Application in NASA IFloodS Field Campaign," J. Hydrometeor., vol. 18, pp. 917-937, April 2017.

[2] H. Chen and V. Chandrasekar, "The quantitative precipitation estimation system for Dallas–Fort Worth (DFW) urban remote sensing network," J. Hydrol., vol. 531, pp. 259-271, 2015.

[3] A. Y. Hou, R. K. Kakar, and Coauthors, "The Global Precipitation Measurement Mission," Bulletin of the American Meteorological Society, vol. 95, no. 5, pp. 701–722, 2014.

[4] R. M. Beauchamp, V. Chandrasekar, H. Chen, and M. Vega, "Overview of the D3R Observations during the IFloodS Field Experiment with Emphasis on Rainfall Mapping and Microphysics," Journal of Hydrometeorology, vol. 16, no. 5, pp. 2118–2132, 2015.

[5] V. Chandrasekar, H. Chen, R. M. Beauchamp, M. Vega, and Coauthors, "Deployment and Performance of the NASA D3R during GPM IFloodS Field Campaign," Proc. of 2014 IEEE International Geoscience and Remote Sensing Symposium (IGARSS), Quebec City, Canada.

[6] V. Chandrasekar, R. M. Beauchamp, H. Chen, M. Vega, and Coauthors, "Deployment and Performance of NASA D3R during GPM IPHEx Field Campaign," Proc. of 2015 IEEE International Geoscience and Remote Sensing Symposium (IGARSS), Milan, Italy.

[7] V Chandrasekar, R. M. Beauchamp, H. Chen, and Coauthors, "Deployment and Performance of the NASA D3R during the GPM OLYMPEx Field Campaign," Proc. of 2016 IEEE International Geoscience and Remote Sensing Symposium (IGARSS), Beijing, China.

[8] V. Chandrasekar; R. M. Beauchamp, M. A. Vega, and H. Chen, "Meteorological Observations and System Performance from the NASA D3R's First 5 Years," Proc. of 2017 IEEE International Geoscience and Remote Sensing Symposium (IGARSS), Fort Worth, Texas.

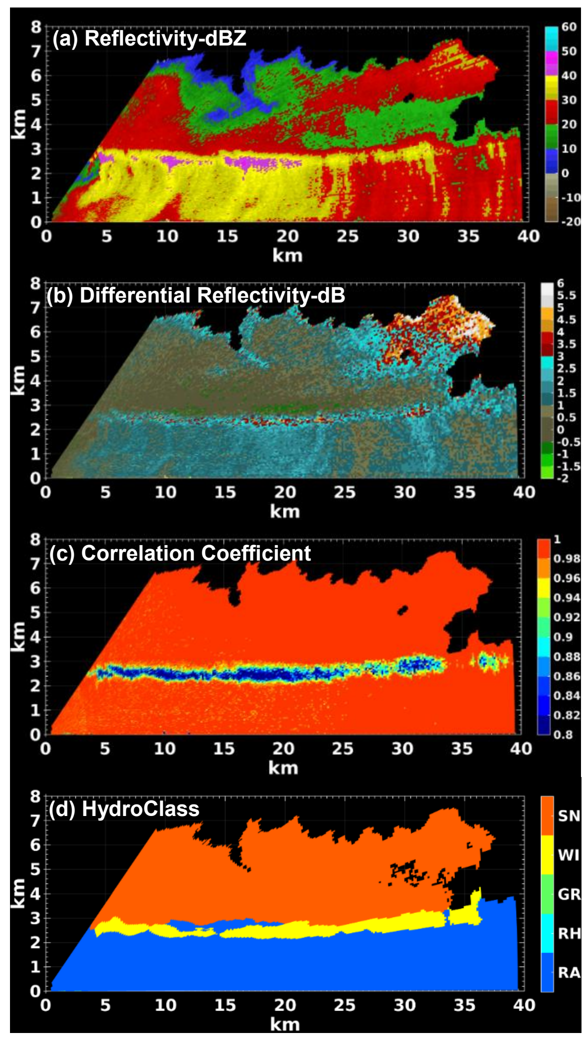

Fig. 3. NASA D3R Ku-band observations and corresponding hydrometeor classification results on June 05, 2013, at 1224UTC: (a) Z_h, (b) Z_{dr}, (c) ρ_{hv}, and (d) classified hydrometeor types. The Z_h and Z_{dr} shown here are after attenuation correction.